

Transactions, SMiRT-26
Berlin/Potsdam, Germany, July 10-15, 2022
Division III

ANALYTICAL STUDY ON BEHAVIOUR OF RC PANELS COVERED WITH STEEL PLATE SUBJECT TO MISSILE IMPACT

Takaaki Tsukada¹, Shin Kuramoto¹, Yasuhiro Ohashi¹

¹ Nuclear Projects Division, Shimizu Corporation, Kyobashi Chuo-ku, Tokyo, JAPAN
(t.tsukada@shimz.co.jp)

ABSTRACT

Experimental study on the behaviour of concrete panels covered with steel plate subjected to missile impact was conducted by many researchers. One of the previous studies [Hashimoto et al. (2005)] confirmed the improvement of impact resistance performance by installing the steel plate at the rear surface of reinforced concrete (RC) panel. In the previous study, the formula was also proposed to evaluate the perforation velocity of non-deformable and deformable missiles against the half steel concrete (HSC) panels in accordance with the energy absorption mechanism of crushed concrete and deformation of steel plate. In the proposed formula, the energy absorption capacity of concrete panel was estimated based on the scabbing impact velocity of concrete panel [W. S. Chang (1981)] and the energy absorption capacity of steel plate was estimated from the experimental results. However, analytical study on the energy absorption mechanism of HSC subject to missile impact has not been conducted in the previous study.

In this study, since the absorbed energy by crushed concrete and steel plate can be computed through the impact simulation based on the six components of stress and strain, analytical study on the energy absorption mechanism is conducted. In the following the investigation on the energy absorption based on the analysis results, the impact simulation by using three-dimensional finite element (FE) models is validated to demonstrate the local failure of RCs and HSCs by comparing the failure modes to the experimental results. Another purpose of this study is to propose the criteria of perforation due to the fracture of steel plate at the rear surface of HSC panels based on the investigation on the energy absorption mechanism.

INTRODUCTION

The necessity to design nuclear-related facilities for an extreme load condition, such as accidental aircraft crash or unexpected terrorist attack, is well recognized for social importance. A reinforced concrete panel has usually been used with the nuclear-related facilities and several methods to improve damage resistance of reinforced concrete panels have been recommended.

Many studies have been conducted on the resistance of reinforced concrete panels subjected to missile impact. As for the local damage of reinforced concrete panel, several formulae were proposed for thickness of a reinforced concrete panel needed to prevent perforation or scabbing on its rear face [(W. S. Chang (1981), NDRC (1946), P. Degen(1980) and P. Degen(1985)).

The reinforced concrete covered with steel plate is expected to be a good impact resistance structure, since steel plate covering the rear surface of concrete is effective to prevent a projectile from perforating the wall and crushed concrete from scattering away. Hence, application of HSC could be one of strong options effective to decrease in thickness of a wall or a roof against missile impact.

Experimental research was conducted to evaluate the impact resistance performance of HSCs in the previous study [Hashimoto et al. (2005)] and the local damage criteria for HSCs were proposed. However, the energy absorption mechanism of HSC subject to missile impact has not been investigated analytically.

The objective of this paper is to demonstrate the various experimental results conducted by Hashimoto to perform analytical study on the energy absorption mechanism by crushed concrete and deformation of steel plate. Another purpose is to propose the perforation criteria on steel plate installed at the rear surface of concrete based on the analysis results in this study.

IMPACT TEST RESULTS

8 and 16 impact specimens were tested for RCs and HSCs, respectively in Hashimoto et al. (2005). The details of specimens are shown in Figure 1. All specimens in series of RCs and HSCs were reinforced with deformed bars of 6.35mm diameter at spacing of 100mm. In a series of HSCs, the steel plates of 750mm square were fixed on the rear surface of RC panels with stud bolts (M3). Here, the spacing of stud bolts was 50mm. The compressive strength of the concrete used in this experiment is 30MPa. A coarse aggregate with maximum size of 10mm was used. The specimens were prepared with five different thicknesses; 60mm, 80mm, 100mm, 120mm and 150mm. The thicknesses of steel plate used for HSCs were 0.5mm, 0.8mm, and 1.2mm. The RC and HSC panels are hanged in the air in the impact test. The missile projectile is non-deformable as shown Figure 2. The typical failure modes of RC and HSC are shown in Figure 3.

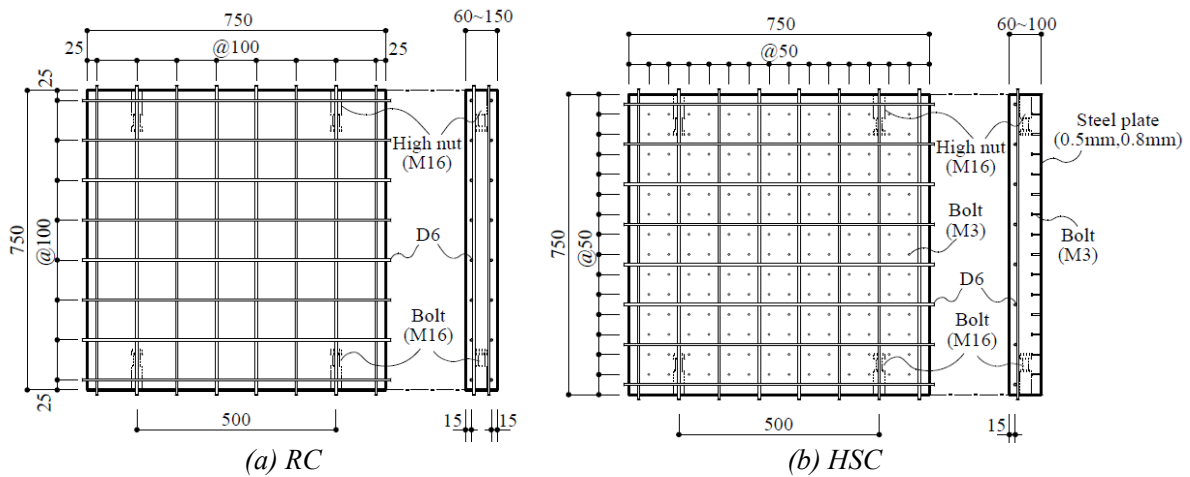


Figure 1. Test specimens

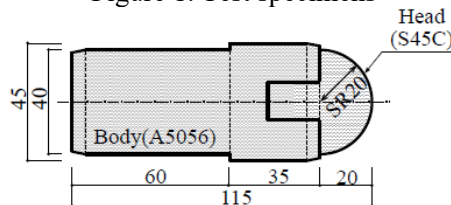


Figure 2. Non-deformable missile projectile

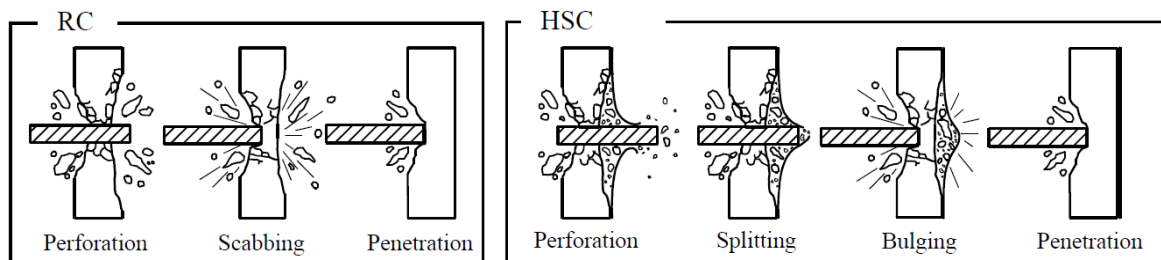


Figure 3. Typical failure mode of RC and HSC panel

ANALYSIS CONDITIONS

The impact analysis model is shown in Figure 4. Concrete panel is modelled by solid elements to assess local damage due to the impact of non-deformable missile. The steel plate installed at the rear surface of panel for HSCs is modelled by shell elements. The studs and reinforcements are modelled by bar elements. The nodes of steel panel, stud and reinforcement model are shared with those of concrete model.

The compressive strength of concrete considered in the impact analysis is 30MPa in accordance with the impact test condition. Material model for concrete is the Karagozian & Case (K&C) concrete model verified in Crawford et al. (2011) which is already implemented in LS-DYNA. Based on the relationship between volumetric strain and hydrostatic pressure, the shear failure surface is defined by the yield failure surface, the maximum failure surface and the residual failure surface. The softening of concrete in compression and tension are modelled as shown in Figure 5 based on the isotropic damage function depending on the effective plastic strain.

As shown in Figure 6, dynamic increase factors are considered as function of strain rate for compression by the approach of the CEB Model Code (2013) and for tension by the modified CEB formulation proposed in Malvar et al. (1998).

Material model for steel plates and reinforcements is chosen to be a piecewise linear plasticity model that allows the definition of an arbitrary stress versus strain curve. Properties of steel plate and reinforcement considered in the analysis in compliance with the impact tests are considered in the analysis as shown in Table 1. To demonstrate the fracture of steel plate, the element erosion criteria is considered according to their average elongation at fracture obtained from material testing with triaxiality factor (TF = 2) for biaxial tension. The studs and missile are supposed as a linear elasticity model.

Element erosion is considered only for steel plate when its strain reached to elongation at fracture divided by TF. Element erosion for concrete is not considered because the concrete loses stiffness for bonding when it is damaged.

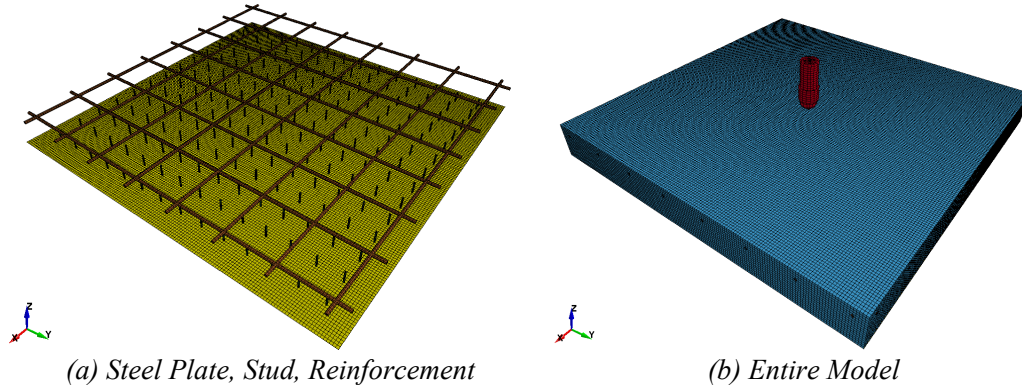


Figure 4. Impact analysis model

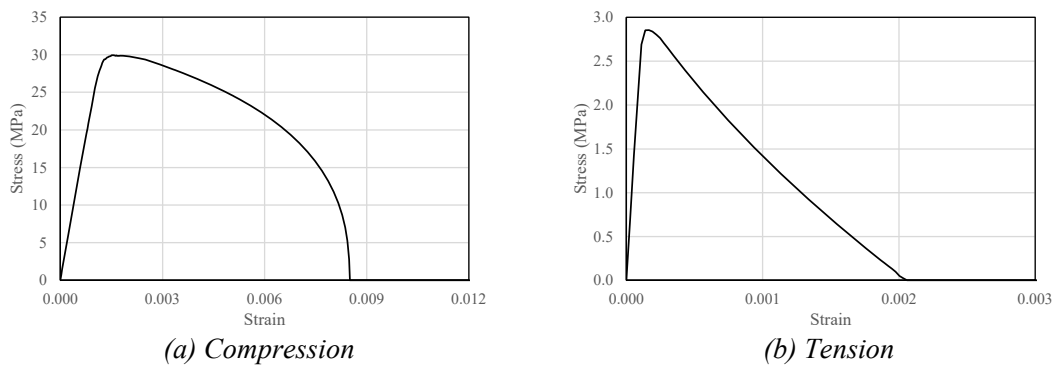


Figure 5. Relationship between stress and strain for concrete

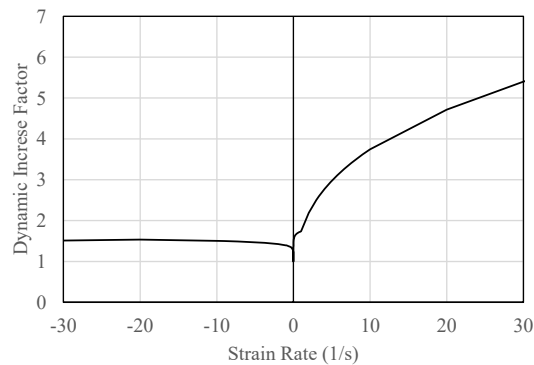


Figure 6. Relationship between dynamic increase factor and strain rate (positive in tension)

Table 1: Properties of steel material

Material		Yield Strength (MPa)	Tensile Strength (MPa)	Elongation at Fracture (%)	Strain Rate Effect (Cowper-Symonds Model)	
					C	P
Steel Plate	0.5mm	213	326	33.3	-	-
	0.8mm	211	303	39.8	-	-
	1.2mm	215	330	35.8	-	-
Reinforcement		345	600	20.0	40	5

ANALYSIS RESULT

Comparisons of typical failure modes between experimental and analytical results are shown in Table 2. The failure modes resulted in the analyses for RCs are judged based on the region of scattering concrete keeping velocity in the end of analysis after impact. For failure mode ‘perforation’, the region of scattering concrete completely through the panel thickness after impact. For ‘scabbing’, the region of scattering concrete is limited only covering concrete at the rear surface of panel. For ‘penetration’, there is no scattering area at the rear surface of panel.

The failure modes resulted in the analyses for HSCs are judged based on the region of fractured steel plate after impact. For ‘perforation’, the region of fractured steel plate is larger than the projectile area of missile and scattering concrete keeps velocity after impact. For ‘splitting’, the region of fractured steel plate is smaller than the projectile area of missile. For ‘Bulging’, no splitting is occurred on the steel plate.

Table 3 summarises the comparison of failure modes between experimental and analytical results to verify the modelling of RC and HSC panels. The analysis results show good agreement with the experimental results. Table 3 also shows the energy calculated in the analysis.

With regard to the RCs, the failure mode of analysis result for RC-N-8 is different from that of experimental result. Considering the failure mode of test case RC-N-7 is perforation and the required thickness to prevent scabbing based on the Chang’s formula is 182mm with reduction factor $\alpha_s = 0.55$ and 100mm with $\alpha_s = 1.00$, the analysis result is considered to be reasonable. In reference to the HSCs, the failure modes obtained from the impact analyses for HSC-N-7 and HSC-N-8 are different from those of the experimental results. As shown in Figure 7 which is perforation criteria for HSCs reproduced from the previous experimental study [Hashimoto et al. (2005)], since the plot of HSC-N-7 and HSC-N-8 (concrete thickness $T=60\text{mm}$ and impact velocity $V=175\text{m/sec}$) are plotted on the line of perforation criteria, the differences between the analytical and experimental results for these specimens are considered to be acceptable..

Table 2: Comparisons of typical failure mode between experimental and analytical results

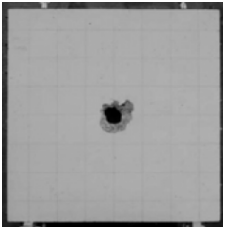
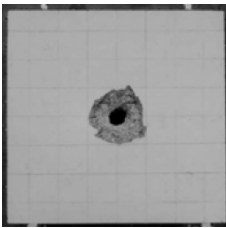
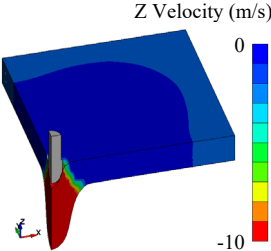
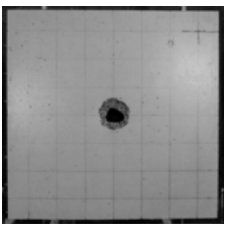
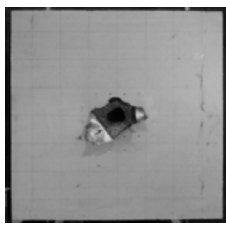
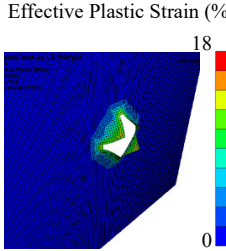
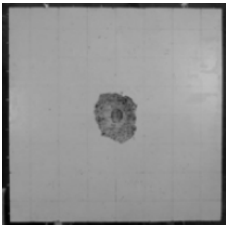
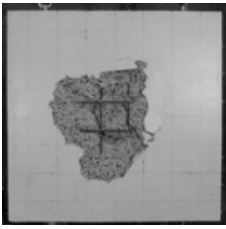
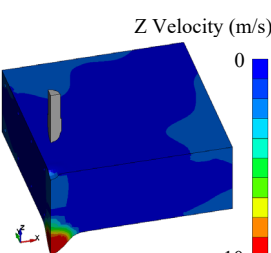
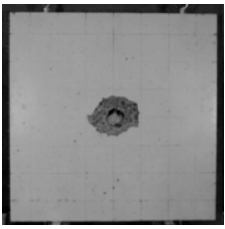
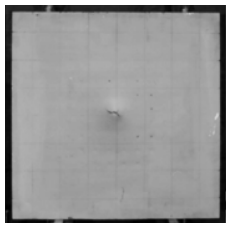
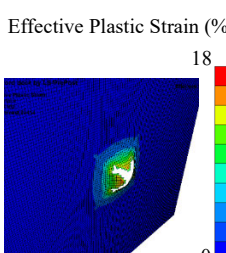
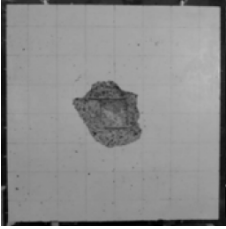
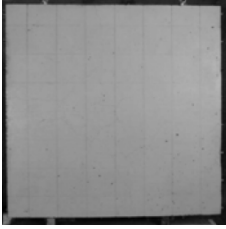
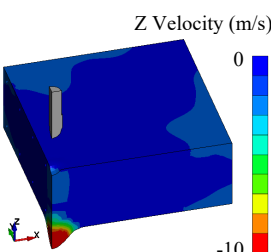
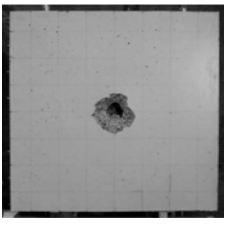
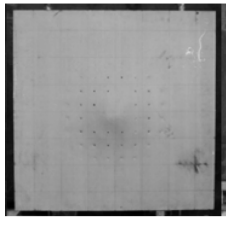
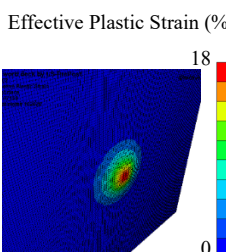
		RC			HSC		
	Experimental Result		Analysis Result	Experimental Result		Analysis Result	
	Front	Rear		Front	Rear		
Perforation	RC-N-1			HSC-N-3			
							
Scabbing	RC-N-6			HSC-N-16			
							
Penetration	RC-N-8			HSC-N-11			
							

Table 3: Comparison of failure mode between experimental and analytical results

Test Case	Impact Test			Impact Analysis					
	Test Parameter			Failure Mode	Failure Mode*1	Initial Kinematic Energy of Missile (J)	Absorbed Energy (J)		Kinematic Energy of Panel After Impact (J)
	Concrete Thickness (mm)	Steel Plate Thickness (mm)	Target Velocity (m/sec)				Concrete	Steel Plate	
RC-N-1	60	0.5	175	Perforation	Perforation	7446	6844	347	
RC-N-2	80		175	Perforation	Perforation	7446	7169	118	
RC-N-3	100		175	Scabbing	Scabbing	7446	7096	71	
RC-N-4	100		215	Perforation	Perforation	11240	10771	138	
RC-N-5	100		215	Perforation	Perforation	11240	10762	137	
RC-N-6	120		215	Scabbing	Scabbing	11240	10607	98	
RC-N-7	120		250	Perforation	Perforation	15200	14443	151	
RC-N-8	150		250	Penetration	Scabbing	15200	14286	110	
HSC-N-1	60	0.5	140	Splitting	Splitting	4766	4445	184	37
HSC-N-2	80		140	Bulging	Bulging	4766	4511	129	32
HSC-N-3	60		175	Perforation	Perforation	7446	6786	225	184
HSC-N-4	80		175	Bulging	Bulging	7446	6993	241	87
HSC-N-5	80		215	Perforation	Perforation	11240	10589	260	161
HSC-N-6	100		250	Bulging	Bulging	15200	14451	307	97
HSC-N-7	60		0.8	175	Bulging	Perforation	7446	6755	322
HSC-N-8	60	175		Bulging	Perforation	7446	6759	318	125
HSC-N-9	80	175		Bulging	Bulging	7446	6963	280	80
HSC-N-10	60	215		Perforation	Perforation	11240	9932	381	418
HSC-N-11	80	215		Bulging	Bulging	11240	10568	404	90
HSC-N-12	80	250		Perforation	Perforation	15200	14158	432	279
HSC-N-13	100	250		Bulging	Bulging	15200	14380	361	104
HSC-N-14	80	1.2		175	Bulging	Bulging	7446	6973	258
HSC-N-15	80		215	Bulging	Bulging	11240	10511	454	98
HSC-N-16	80		250	Splitting	Splitting	15200	14132	589	175

Note *1: The different failure mode from test result is shaded.

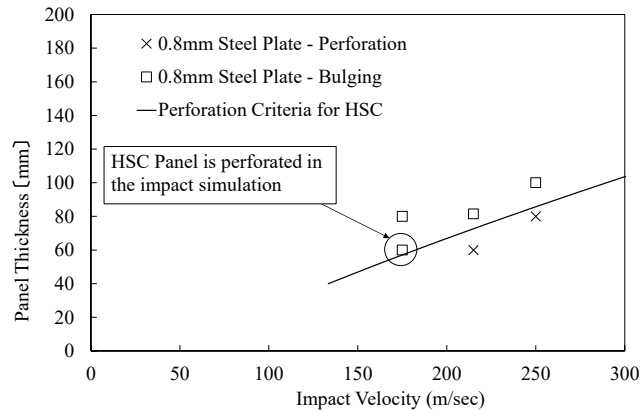


Figure 7. Required HSC panel thickness with 0.8mm steel plate to prevent perforation, (reproduction from [Hashimoto et al. (2005)])

CRITERIA ON FRACTURE OF STEEL PLATE

As shown in Table 3, the kinematic energy of missile is mainly absorbed by crushed concrete. Figure 8 shows relationship between impact velocity and energy absorbed by crushed concrete for all the RCs and the HSCs. Although required HSC thickness to prevent perforation proposed in [Hashimoto et al. (2005)] assumes that the energy absorption capacity of concrete depends on concrete panel thickness and material strength regardless to impact velocity, the analysis results show that the energy absorbed by crushed concrete strongly correlates to the impact velocity which affects the pressure ($=I/3$ where, I is first invariant

of stress tensor) on concrete and strain rate enhancing the resistance of concrete. No significant differences are observed in energy absorption between RCs and HSCs.

To confirm the effect of impact velocity on the energy absorbed by concrete, the out-of-plane shear behaviour are investigated for the representative elements which locate on the out-of-plane shear crack through the concrete panel as shown in Figure 9. The stress – strain relationship is compared with that obtained from single element analysis. As shown in Figure 10, static analyses are conducted with unconfined (pure shear) and confined boundary conditions. The out-of-plane stress – strain relationship and stress path, deviatoric stress ($=\sqrt{3J_2}$ where, J_2 is second invariant of the deviatoric stress tensor) – pressure relationship, with failure surface of the representative elements are investigated in Figure 11 (a) and (b) for analysis cases HSC-14 through HSC-16 (80mm concrete thickness, 1.2mm steel plate thickness and 175, 215, 250 m/sec impact velocities) and RC-N-2 (80mm concrete thickness and 175 m/sec impact velocities). Note that the strain rate effect is not considered for the plotted failure surface. In Figure 11 (c), the stress paths obtained from the additional impact analyses for HSC-14 through HSC-16 by eliminating the strain rate effect are shown in comparison. It is confirmed that the stress paths are always within the failure surface unless strain rate effect is considered. As shown in Figure 11 (b), the rate effect expands the failure surface, which affects the confinement effect for further enhancement of concrete strength. As a result, out-of-plane stress – strain relationship subject to the higher impact velocity shows the wider stress – strain hysteresis curve exceeding the strength obtained from confined single element as shown in Figure 11 (a), which increase the energy absorbed by the crushed concrete.

Figure 12 shows the relationship between residual energy, E_r (= initial kinematic energy of impact missile – energy absorbed by concrete) and the energy absorbed by steel plate in the impact analysis. E_r includes kinematic energy of missile and other components than concrete after impact which is about 5% of total energy in maximum. Since the energy demand to steel plate depends on the contribution area of steel plate, E_r in Figure 12 is divided by assumed contribution area based on Figure 13 (a). The energy absorption performance of steel plate is proportional to the energy demand unless the energy demand exceeds the energy absorption capacity of steel plate and perforation occurs. Therefore, installation of steel plate with higher capacity than the linear approximation in Figure 12 can prevent the impact missile from perforating the HSC.

The failure criteria in terms of energy absorption capacity of steel plate, E_s , are calculated theoretically by equation 1 based on the assumption shown in Figure 13. Based on the analytical results, it is confirmed that the plastic strain distribution is concentric and the gradient of plastic strain is almost constant as shown in Figure 13 (b). The stress – strain relationship is assumed as rigid-perfectly-plastic for simplification as shown Figure 13 (c). The triaxial factor (TF=2) is considered for the strain at fracture. The comparison between theoretical capacity and absorbed energy is shown in Figure 14. Although the theoretical capacity is slightly conservative due to the simplification, the analytical cases in which the energy absorbed by steel plate exceeds the theoretical capacity result in perforation. Therefore, if the energy absorbed by concrete is correctly assumed, the perforation criteria of steel plate can also be evaluated.

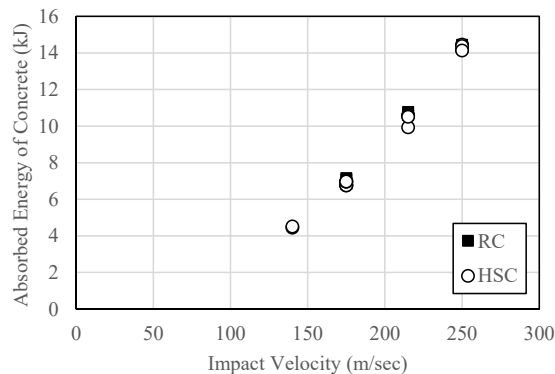


Figure 8. Relationship between impact velocity and energy absorbed by concrete

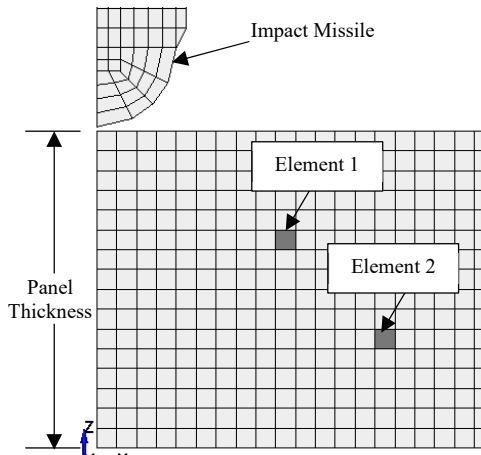


Figure 9. Elements for investigation

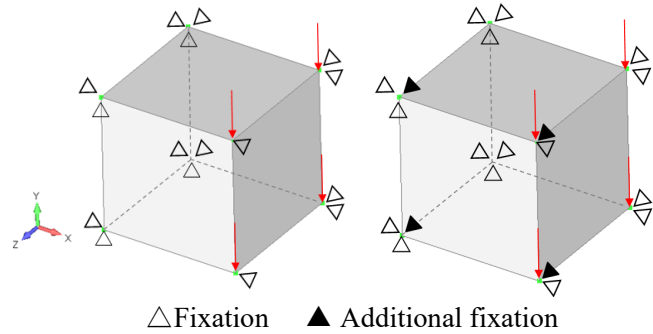
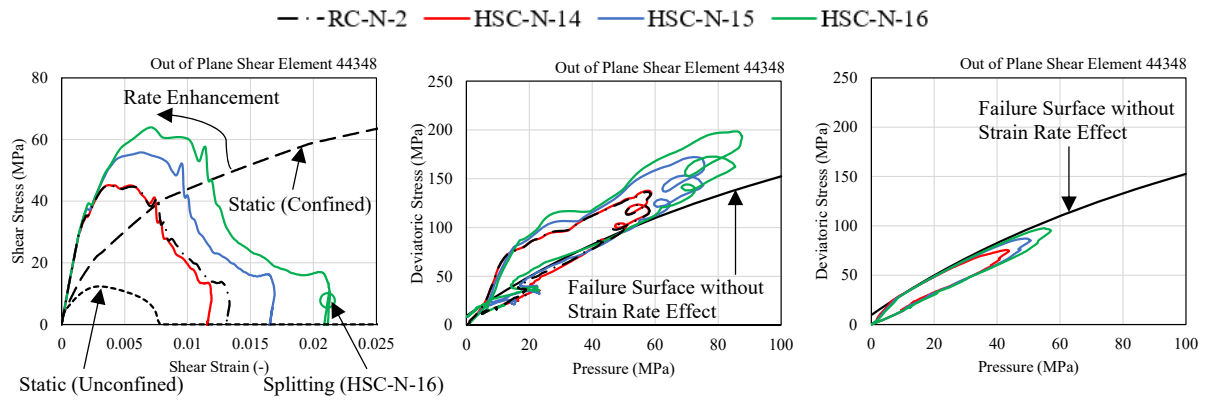


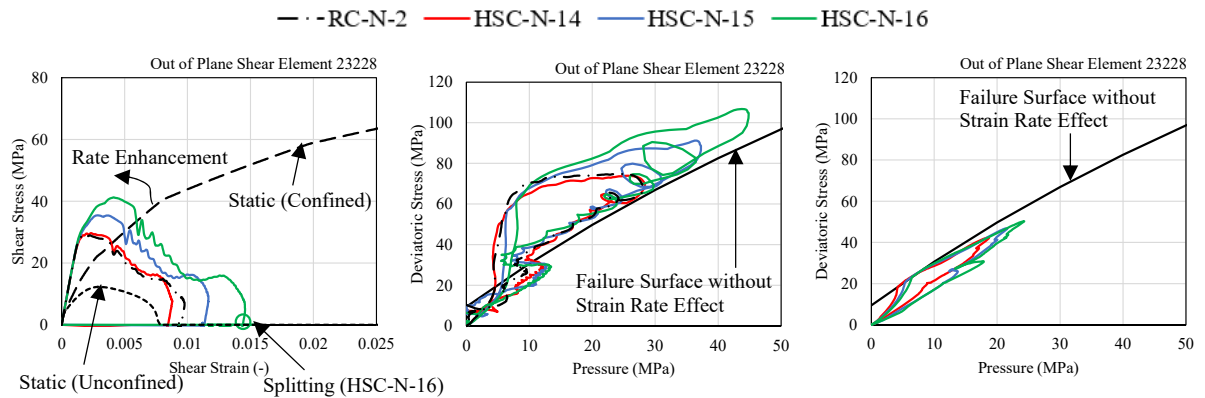
Figure 10. Static shear analysis by single element



(a) Out-of-plane shear stress-strain

(b) Load path
(1) Element 1

(c) Load path without rate effect



(a) Out-of-plane shear stress-strain

(b) Load path
(2) Element 2

(c) Load path without rate effect

Figure 11. Relationship between behaviour of concrete and impact velocity

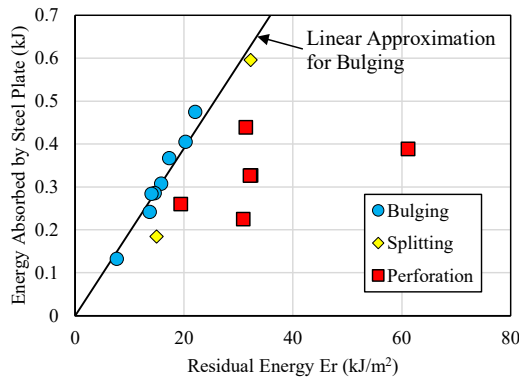


Figure 12. Relationship between residual energy and energy absorbed by steel plate

$$\begin{aligned}
 E_s &= \int_0^{2\pi} \int_0^R \varepsilon_{cr} (1 - r/R) \cdot \sigma_y \cdot T \cdot r \cdot dr \cdot d\theta, \quad R = t + b/2 \\
 &= \frac{1}{3} \pi \cdot \varepsilon_{cr} \cdot \sigma_y \cdot T \cdot R^2
 \end{aligned}
 \tag{1}$$

where, E_s is theoretical energy absorption capacity of steel plate, b is diameter of projectile, T is thickness of steel plate, see Figure 13 for the other parameters.

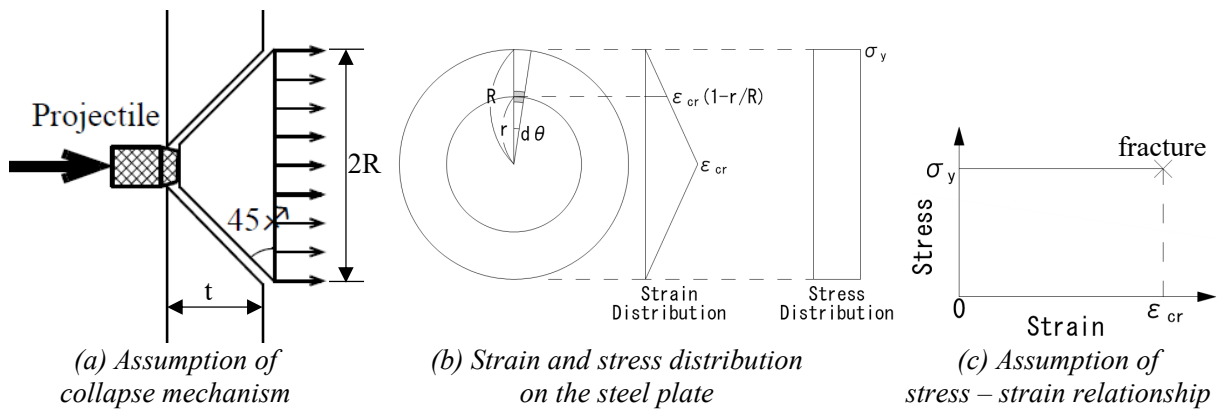


Figure 13. Assumption on calculation of energy absorption capacity of steel plate

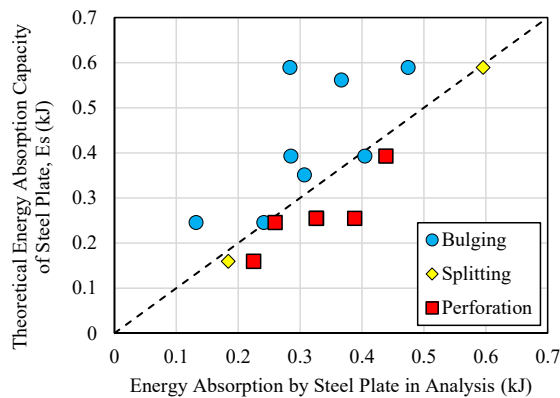


Figure 14. Comparison of energy absorbed by steel plate in impact analysis and theoretical capacity

CONCLUSION

A series of impact analysis on RCs and HSCs subjected to missile impact is conducted to demonstrate experimental study.

The energy absorption mechanism is investigated based on the kinematic energy of missile and calculated absorbed energy by crushed concrete and deformation of steel plate. The absorbed energy of concrete strongly correlated to the impact velocity which affects pressure on the concrete and strain rate enhancing the concrete strength. The energy demand to steel plate to prevent perforation is evaluated by residual energy of kinematic energy of missile subtracted by the absorbed energy of concrete. The analysis results show that the energy demand to steel plate exceeding the theoretical capacity of steel plate causes perforation of the HSC. Therefore, based on the relationship between energy absorbed by concrete and impact velocity, and theoretical capacity of steel plate, the perforation of HSCs is to be prevented.

Energy absorption mechanism is investigated analytically in this study based on the experimental results. Following continuous studies are needed to develop the practical design methodology for HSC with realistic scale of missile projectile and nuclear plant structures against impact missile.

- Additional study considering the realistic scale of nuclear power plants and missiles needs to be conducted to extrapolate the relationship between analytical parameters and results investigated in this study and develop perforation criteria for practical design.
- Additional investigation on the relationship between the energy absorbed by concrete and the weight of impact missile needs to be conducted. Although the correlation between absorbed energy by concrete and impact velocity is confirmed in this study, the weight of impact missile which is another parameter of kinematic energy of impact missile is constant.
- Additional investigation on the relationship between the energy absorbed by concrete and kinematic energy of deformable missile needs to be conducted because the deformation of impact missile affects the energy absorption mechanism and energy demand to the steel plate.

REFERENCES

- J. Hashimoto, K. Takiguchi, K. Nishimura, K. Matsuzawa, M. Tsutsui, Y. Ohashi., I. Kojima and H. Torita (2005). "Experimental Study on Behavior of RC Panels Covered with Steel Plates Subjected to Missile Impact," *18th SMiRT*, J05-4.
- W. S. Chang, "Impact of Solid Missile on Concrete Barriers", *Journal of the Structural Division*, ASCE, Vol.107, No.ST2, pp.257-271.
- National Defense Research Committee (1946), "Effects of Impact and Explosion", *Summary Technical Report of Division 2*, Vol.1, Washington DC.
- P. Degen (1980), "Perforation of Reinforced Concrete Slabs by Rigid Missiles", *Journal of the Structural Division*, ASCE, Vol.106, No.ST7, pp.1623-1642.
- A. Haldar (1985), "Energy-balanced approach to evaluate local effects of impact of non deformable missiles on concrete structures", *8th SMiRT* J6/3.
- Crawford et al. (2011). "Use and Verification of the Release III K&C Concrete Material Mod-el in LS-DYNA" *Karagozian & Case*.
- Comité Euro-International du Béton (2013). "fib Model Code for Concrete Structures 2010" *Ernst & Sohn Verlag*.
- L. Javier Malvar and John E. Crawford (1998). "Dynamic Increase Factors for Concrete" *28th DDESB Seminar at Orlando*.